Drug Design, Development and Therapy

Dovepress
open access to scientific and medical research

Open Access Full Text Article

ORIGINAL RESEARCH

Anti-Breast Cancer Effect of 2-Dodecyl-6-Methoxycyclohexa-2,5-Diene-1,4-Dione in vivo and in vitro Through MAPK Signaling Pathway

This article was published in the following Dove Press journal:
Drug Design, Development and Therapy

Xing Zhou*
Xingchun Wu*
Luhui Qin
Shunyu Lu
Hongliang Zhang
Jinbin Wei
Lixiu Chen
Luhui Jiang
Yani Wu
Chunxia Chen
Renbin Huang

Pharmaceutical College, Guangxi Medical University, Nanning 530021, Guangxi, People's Republic of China

*These authors contributed equally to this work

Background: 2-Dodecyl-6-methoxycyclohexa-2,5-diene-1,4-dione (DMDD) has been reported to inhibit a variety of cancer cell lines. The purpose of this study was to investigate the effects of DMDD on 4T1 breast cancer cells and the effects of DMDD on 4T1 breast cancer in mice and its molecular mechanisms.

Methods: 4T1 breast cancer cells were treated with different concentrations of DMDD, and their proliferation, apoptosis, cell-cycle distribution, migration, and invasion were detected by 3-(4,5-dimethyl-2-thiazolyl)-2,5-diphenyl-2-H-tetrazolium bromide (MTT, Acridine orange and ethidium bromide dual staining analysis (AO/EB) dual staining, flow cytometry, scratch test, and the Transwell assay. Relative quantitative real-time qPCR analysis and Western blot were applied to examine the expression levels of related genes and proteins. In animal experiments, we established a xenograft model to assess the anti-breast cancer effects of DMDD by evaluating the inhibition rate. The apoptotic activity of DMDD was evaluated by hematoxylin-eosin (HE) staining, transmission electron microscope (TEM) analysis and TdT-mediated dUTP nick end labeling (TUNEL) assays. The mRNA expression levels of MAPK pathway components were detected by relative quantitative real-time qPCR. In addition, the protein expression levels of MAPK pathway components were assessed through immunohistochemical assays and Western blotting.

Results: Experiments showed that DMDD could inhibit the proliferation, migration, invasion of 4T1 cells and induce cellular apoptosis and G1 cell cycle arrest. Moreover, DMDD down-regulated the mRNA expressions of raf1, mek1, mek2, erk1, erk2, bcl2, and up-regulated the mRNA expression of bax. DMDD reduced the protein expressions of p-raf1, p-mek, p-erk, p-p38, Bcl2, MMP2, MMP9 and increased the protein expressions of Bax and p-JNK. The results showed that DMDD can effectively reduce the tumor volume and weight of breast cancer in vivo, up-regulate the expression of IL-2, down-regulate the expression of IL-4 and IL-10, induce the apoptosis of breast cancer cells in mice, and regulate the expression of genes and proteins of the MAPK pathway.

Conclusion: Our study indicates that DMDD can inhibit proliferation, migration, and invasion and induces apoptosis and cell-cycle arrest of 4T1 breast cancer cells. Also, our findings indicate that DMDD induces the apoptosis of breast cancer cells and inhibits the growth in mice. Its mechanism may be related to the MAPK pathway.

Keywords: DMDD, breast cancer, MAPK signaling pathway, Bcl-2 family

Correspondence: Renbin Huang; Chunxia Chen
Tel +86 771 5339805
Fax +86 771 5358272
Email huangrenbin518@163.com; Chunxia251401@126.com

Introduction

Breast cancer, one of the most common cancers in women, poses a huge threat to women's physical and mental health and can even endanger life. The global

submit your manuscript | www.dovepress.com
DovePress
http://doi.org/10.2147/DDDT.S237699

incidence of breast cancer has been on the rise.[1,2] Clinically, surgery, radiotherapy, and chemotherapy are selected as conventional treatments according to the stage of the tumor and the physical condition of the patient. However, they do not have a good therapeutic effect and the side effects are large.[3,4]

In recent years, the anti-tumor effects of Chinese medicine monomer components have become a research hotspot at home and abroad. For example, Ginkgo Biloba extract can effectively inhibit metastasis in Gastric Cancer,[5] and Oxymatrine can strengthen the inhibitory effect of bevacizumab on breast cancer.[6] The root of *Averrhoa carambola L.*, which is used as a folk herbal medicine, can lower blood sugar and blood lipids. The form used was identified as the dry root of the Oxalidaceae plant. 2-dodecyl-6-methoxycyclohexa-2,5-diene-1,4-dione (DMDD) which is extracted and isolated from the roots of *Averrhoa carambola L.* is a good active composition.[7] Previous studies have confirmed that its pharmacological effects mainly include antihyperglycemic, regulation of blood lipids, and lessening of inflammation.[8–11] Recent studies have found that DMDD can inhibit the proliferation of various cancer cells[12] and inhibit breast tumor growth in mice.[13] However, its anti-tumor mechanism is still unclear, and further research is needed. The expression of IL-2, IL-4 and IL-10, which are important indicators for evaluating immune function, is closely associated with the occurrence and development of tumors. Some studies have reported that IL-2, IL-4 and IL-10 are abnormally expressed in cancer and can also be used as tumor markers.

The mitogen-activated protein kinase (MAPKs) signaling pathway is not only involved in the regulation of various physiological processes of cells, including cell growth, differentiation, and death but also closely related to the occurrence and development of tumors.[14–16] Extracellular signal-regulated protein kinase (ERK), c-Jun amino-terminal kinase (JNK), and P38 MAPK are the three main subpathways of the (MAPKs) pathway.[17,18] Previous studies have shown that various tumor cell behavioral activities are closely related to abnormal activation or abnormal inhibition of MAPKs.[19,20] Therefore, the MAPKs pathway may be a potential target for tumor therapy.[21]

In recent years, 4T1 breast cancer cell model and 4T1 breast cancer mouse model have been widely used in the research of chemotherapy, Chinese herbal medicine monomer and biological therapy against breast cancer.[22,23] Therefore, in this experiment, these two models were selected to study the anti-breast cancer effect of DMDD and related mechanisms.

Materials and Methods

Plant Materials and Extraction and Isolation of DMDD

The roots of *Averrhoa carambola L.*, identified as dry roots of the Oxalidaceae plant by Prof Maoxiang Lai (Traditional Chinese Medicine Research Institute of Guangxi), were picked from the Lingshan County of Guangxi, China. After being picked back, the roots were dried and made into a coarse powder. The extraction, isolation, and identification of DMDD were performed according to the methods previously described.[7–9] The purity of DMDD is about 95%. A 10 mM stock solution of DMDD was prepared using dimethyl sulfoxide (DMSO, cell culture grade, Solarbio, Beijing, China) as a solvent for DMDD, and it was further diluted in the cell culture medium before administration. The Chemical structure of DMDD is shown in Figure 1.

Cell Culture

4T1 breast cancer cells (4T1 cells, murine-derived breast cancer cell lines) were bought from the Shanghai Cell Bank of the Chinese Academy of Sciences. The medium of the cells consisted of RPMI-1640 media (GIBCO, New York, USA), 10% fetal bovine serum (FBS, GIBCO, New York, USA) and 1% penicillin-streptomycin (Solarbio, Beijing, China). The conditions of the cell incubator were 37°C with 5% CO_2.

Cell Proliferation Analysis

4T1 cell proliferation ability was detected by MTT assay. 100 μL of culture medium with 0.3×10^4 cells was put into each well of a 96-well plate overnight and then given various concentrations of DMDD. After incubation for 24 hours and 48 hours, 15 μL of MTT (5mg/mL, Solarbio, Beijing, China) was put into each well and then cultivating for 4 hours. Finally, 150 μL dimethyl sulfoxide (DMSO, AR,

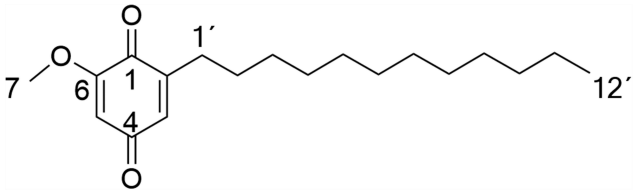

Figure 1 Chemical structure of DMDD.

Solarbio, Beijing, China) was put into each well and dissolve the purple crystal sufficiently. The absorbances were detected by a microplate reader (Thermo, UK). Cell inhibition rates were calculated.

Cell Colony Formation Assay

4T1 cells were divided into the control group, DMDD L group, DMDD M group, and DMDD H group. Different groups of cells were given the corresponding concentrations of DMDD and cultured for 24 hours. Then, the cells of each group were collected separately. One milliliter of culture medium with 3×10^2 cells was put into each well of a 6-well plate and cultured under standard conditions. Two weeks later, the cells on the plates were fastened with methanol (Kelong, Chengdu, China) for 30 minutes and dyed using crystal violet (0.1%, Solarbio, Beijing, China) for 30 minutes. The colony-forming units were photographed and cell colonies were counted.

Acridine Orange and Ethidium Bromide Dual Staining Analysis

AO/EB (Solarbio, Beijing, China) dual staining analysis was conducted to detect the morphological changes of apoptotic cells. 4T1 cells were digested and 1 mL of culture medium with 1×10^5 cells was put into each well of a 6-well plate cultivating for 24 hours in an incubator with 37°C, 5% CO_2 overnight. Then, different groups of cells were given the corresponding concentrations of DMDD and cultured for 24 hours. Cells were washed using PBS (pH 7.4, Solarbio, Beijing, China) twice. According to the kit instructions, cells were stained with AO/EB stain. The cells were observed with a fluorescent microscope (Olympus, Japan) and pictures were taken.

Cell Apoptosis Analysis

4T1 cells were digested, and 1 mL of culture medium with 2×10^5 cells was put into each well of a 6-well plate cultivating for 24 hours in an incubator with 37°C, 5% CO_2 overnight. Then, different groups of cells were given the corresponding concentrations of DMDD and cultured for 24 hours. The rate of cell apoptosis was evaluated with the Annexin V-FITC/ PI Apoptosis detection kit (KeyGEN BioTECH, Nan Jing, China) by a flow cytometer (Becton Dickinson, NJ, USA).

Cell Cycle Analysis

4T1 cells were digested, and 1 mL of culture medium with 3×10^5 cells was put into each well of a 6-well plate cultivating for 24 hours in an incubator with 37°C, 5% CO_2 overnight. Then, different groups of cells were given the corresponding concentrations of DMDD and cultured for 24 hours. Cells were collected and fixed with ethanol at a final concentration of 70% overnight. Next, PBS was used to wash cells to remove ethanol. Finally, cells were stained with a PI solution of a cell cycle detection kit (Technologies, Carlsbad, CA, USA) and protected from light for 15 minutes at room temperature. A flow cytometer was used to analyze cell-cycle distribution.

Scratch Test

Cell migration ability was detected by the Scratch test. 4T1 cells were digested, and 1 mL of culture medium with 2×10^5 cells was put into each well of a 24-well plate cultivating for 24 hours in an incubator with 37°C, 5% CO2. After the cells are full, the scratch wound was created on the cells in the center of every well with a 100 μL pipette tip. Then, different groups of cells were given the corresponding concentrations of DMDD and cultured for 24 hours. At last, cell migrations over the wound area were observed and imaged with an inverted optical microscope (Olympus, Japan). Cell migration rates were calculated.

Transwell Assay

Matrigel (Corning, USA) was diluted with the serum-free medium (4°C pre-cooled) in a ratio of 1:4. Transwell chambers (8 μm pore size, Corning, USA) were coated with 50 μL of the diluted Matrigel and then put in an incubator with 37°C for 1 hour to make it gelatinous. Then, a 200 μL non-serum culture medium with a corresponding concentration of DMDD that contained 5×104 cells was put into each chamber. Meanwhile, 800 μL culture medium with 15% FBS was added into each well of a 24-well plate, and the transwell chambers were put into the 24-well plate. After culturing for 24 hours, PBS was used to wash the upper chambers to remove the cells on the upper side of the chambers. Methanol was used to fix the cells on the lower side of the chambers, and crystal violet (0.1%) was applied to dye the cells for 30 minutes at room temperature. After washing and drying, the stained cells are the cells that invade the lower chamber. Four fields were randomly selected for calculation of relative invasion under an inverted microscope (×400).

The Relative Quantitative Real-Time PCR Analysis

Different groups of cells were given the corresponding concentrations of DMDD and cultured for 24 hours, and then different groups of 4T1 cells were separately digested and collected into centrifuge tubes. AxyPrep Multisource Total RNA Miniprep Kit (Axygen, China) was used to extract the total RNA. The nucleic acid analyzer was then conducted to detect the concentration of the total RNA. Next, the 5X PrimeScript RT Master Mix kit (Takara, Beijing, China) was applied to reverse-transcribe RNA into cDNA. Finally, 7300 real-time thermocyclers (Applied Biosystems, Foster City, CA, USA) were performed to detect the expression levels of the genes. GADPH was used as an internal reference. Results were calculated using the $2^{-\Delta\Delta Ct}$ method. Related primer information is shown (Table 1).

Western Blotting Analysis

Different groups of cells were given the corresponding concentrations of DMDD and cultured for 24 hours, and then different groups of 4T1 cells were separately digested and collected into centrifuge tubes. Highly efficient RIPA tissue/cell rapid lysate (Solarbio, Beijing, China) was mixed with PMSF (Solarbio, Beijing, China) and a protease inhibitor cocktail (CWBIO, Beijing, China) at a ratio of 100:1:1 and the mixture were used to extract proteins from 4T1 cells. BCA Protein Assay kit (Beyotime, Shanghai, China) was applied to detect the protein concentration. Protein samples (50 μg) were electrophoresed on SDS-PAGE gels (10%), and protein signal was transferred onto PVDF membranes (ISEQ00010; Millipore, Billerica, MA, USA) by electroblotting. The membranes were soaked in primary antibodies at 4°C overnight and then soaked in secondary antibody for 1 hour at room temperature on the shaker. Primary antibodies included p-raf1, raf1, p-mek, mek, perk, erk, p-JNK, JNK, p-p38, p38, Bcl2, Bax, MMP2, MMP9 and GAPDH (all from Cell Signaling Technology, MA, USA). The ratio of all primary antibody to diluent is 1:1000. Secondary antibody was anti-rabbit (5366P) IgG(H+L) (DyLight(TM)) antibodies (1:10,000). Reactive bands of the membranes were detected using a near-infrared two-color fluorescence imaging system (LI-COR Odyssey CLx). GADPH was used as an internal reference.

Animals and Reagents

BALB/c mice (female, 6-8 weeks, 18-22 g) were purchased from Changsha Tianqin Biotechnology Co., Ltd. Doxorubicin hydrochloride (cat. no. 1801E2) was purchased from Shenzhen Main Luck Pharmaceuticals Inc. All experiments were performed with approval from the Institutional Animal Care and Use Committee of Guangxi Medical University. Animal ethics review follows the Guiding Opinions on the Treatment of Laboratory Animals issued by the Ministry of Science and Technology of the People's Republic of China and the Laboratory Animal-Guideline for Ethical Review of Animal Welfare issued by the National Standard GB/T35892-2018 of the People's Republic of China. A Mouse SP Kit was purchased from ZSGB-BIO Technology Co., Ltd. IL-2, IL-4 and IL-10 ELISA kits (cat. no. 03/2019) were obtained from Shanghai Fanke Industrial Co., Ltd. A TUNEL Apoptosis Detection kit (cat. no.11684817910) was purchased from Roche. Antibodies against RAF1 (cat. no. 53745), p38 (cat. no. 8690T), p-ERK (cat. no. 4370S), p-p38 (cat. no. 4511T) and rabbit IgG(H+L) (cat. no. 5366P) were obtained from Cell Signaling Technology, Inc. ERK (cat. no. 184699), MEK (cat. no. 178876), p-MEK (cat. no. 194754) and p-RAF1 (cat. no. 173539) antibodies were obtained from Abcam. JNK (cat. no. WL01295), p-JNK (cat. no. WL01813), Bcl-2 (cat. no. WL01556) and Bax (cat. no. WL01637) antibodies were obtained from Wanleibio.

Table 1 Primer Information for the RT-PCR

Gene	Forward Primer (5'-3')	Reverse Primer (5'-3')
raf1	ACTGTGGTCAATGTGCGGAATGG	GGCGGCATCGGTGTTCCAATC
mek1	GACTTTGAGAAGATCAGCGAAC	GTTTGATCTCCAGGTGGATCAG
mek2	CATCAGTGTAGGTCATGGGATG	GTGGCTCGTTCACTATGTAGTC
erk1	ATCTCAACAAAGTTCGAGTTGC	GTCTGAAGCGCAGTAAGATTTT
erk2	CTGCTGGACCGGATGTTAACCTTC	ACTGGCTCATCTGTCGGATCGTAG
bcl2	GATGACTTCTCTCGTCGCTAC	GAACTCAAAGAAGGCCACAATC
bax	TTGCCCTCTTCTACTTTGCTAG	CCATGATGGTTCTGATCAGCTC
GAPDH	GGTTGTCTCCTGCGACTTCA	TGGTCCAGGGTTTCTTACTCC

Establishment of 4T1 Breast Cancer Mouse Model and Animal Administration

4T1 cells were cultured in large quantities and digested when they reached the logarithmic growth phase. BALB/c mice were transplanted subcutaneously into the right axilla with 0.1 mL of cell suspension containing 1×106 4T1 cells to establish the subcutaneous xenograft mouse model of breast cancer. The weight of mice and the growth of tumors were measured daily. When the tumors grew to 100 mm3 in size, the mice were randomly divided into five groups: the DMDD-H group (DMDD 100 mg/kg, qd, ig), the DMDD-M group (DMDD 50 mg/kg, qd, ig), the DMDD-L group (DMDD 25 mg/kg, qd, ig), the DOX group (doxorubicin 0.5 mg/kg, qw, ip) and the model group, with 10 mice in each group. In addition, 10 mice without tumor cells were selected as the normal group. Mice were treated for 14 days, with tumor volume and weight were measured every two days. Tumor volume was calculated as (width2 × length)/2. The inhibition rate of tumor growth was calculated as (%)= (Mean tumor weight of vehicle group − Mean tumor weight of treatment group)/Mean tumor weight of vehicle group × 100%. In addition, the liver index = liver weight (mg)/body weight (g), and the spleen index = spleen weight (mg)/body weight (g).

Detection of Cytokines in Serum

ELISA kits were used to determine the levels of cytokines (IL-2, IL-4 and IL-10) in the serum samples. The procedure for the experiment was carried out according to the kit instructions.

HE Staining

One-quarter of the mouse tumors were immersed in 4% formaldehyde for 24 hours and then dehydrated, waxed and sliced. The sections of each group were dewaxed and stained with hematoxylin and eosin solution, after which the pathological changes in the structure of the tumors were observed.

Observation of Ultrastructure of Tumor Tissue

The model, DOX and DMDD-H groups were selected for TEM analysis. The mice were sacrificed, 1 mm3 of tissue was quickly removed from the tumors, fixed with 3% glutaraldehyde for more than 2 hours and then immobilized with 1% osmium acid for 1 to 2 hours. The tissues were dehydrated step by step with ethanol and acetone and then soaked overnight with acetone and embedding agent. Finally, the tissues were observed by TEM (Hitachi, H-7650) after they were embedded, polymerized, repaired, sliced and double stained with uranium acetate and lead citrate.

TUNEL Assay

A FITC fluorescein labeling kit was used to determine the number of apoptotic cells in the 4T1 xenografts. The staining was performed on paraffin sections according to the manufacturer's instructions. DAPI was used to stain the nucleus blue, while TUNEL staining caused the nucleus to appear green. TUNEL-positive cells with green staining of the nucleus from three random fields (400×) in each section were counted. The formula used to calculate the apoptotic index was positive cells/total cells ×100%.

Relative Quantitative Real-Time qPCR

Real-time qPCR was performed to detect the level of RAF1, MEK, ERK, Bcl-2 and Bax gene expression. Total RNA was extracted using a Total RNA Miniprep kit (AXYGEN Biotechnology Co. Ltd, Hangzhou, China) following the manufacturer's instructions. Next, cDNA was synthesized from the RNA with PrimeScript RT Master Mix (Perfect Real Time) (Takara Biotechnology Co. Ltd, Dalian, China). The quantity of the mRNA was measured using a PowerUp™ SYBR™ Green Master Mix kit (Thermo Fisher Scientific Co. Ltd, MA, USA) and was performed in an ABI Prism 7300 real-time thermocycler (Applied Biosystems, Foster City, CA, USA). GAPDH was selected as an endogenous control. The 2-DDCTmethod was used for analysis. Sequence-specific primers are shown in Table 1.

Immunohistochemical Assay

Immunohistochemistry analysis was performed to detect the expression of p-RAF1, p-MEK and p-ERK in tumor tissues. The slices were dewaxed and the antigen was repaired with citric acid solution (0.01 mol/L, pH 6.0), after which the slices were incubated with 3% H2O2. The slices were blocked with non-immunoreactive sera and then incubated with antibodies against p-RAF1, p-MEK and p-ERK overnight at 4°C. The next day, the slices were incubated with goat anti-rabbit (HRP), stained with DAB chromogen and counterstained with hematoxylin. The slices were observed and analyzed using a light microscope (Olympus, Tokyo, Japan). Immunohistochemical positive

expression was evaluated by calculating the IOD value through an analysis with Image-Pro Plus 6.0.

Western Blotting

Western blotting was performed to analyze the expression of MAPK signaling pathway-related proteins and two apoptotic proteins in the tumor tissues of mice. Proteins were extracted from tumor tissue by grinding with liquid nitrogen and adding lysis buffer, PSMF and phosphatase inhibitors. Equal amounts of proteins were mixed with 4× loading buffer after measuring the protein concentrations using a BCA assay. The proteins were separated by 10% SDS-PAGE and then transferred to a PVDF membrane. Subsequently, the membranes were blocked with 5% non-fat milk for 1 h and then incubated with primary antibodies overnight at 4°C. Then, the membranes were incubated with the anti-rabbit IgG (H+L) secondary antibodies at room temperature for 1 h. The Western blotting results were detected and analyzed using Image Studio Lite.

Statistical Analysis

SPSS 17.0 software was used to analyze results. All data were presented as mean ± standard deviation (n=3). One-way analysis of variance (ANOVA) was performed to compare the differences between experiments and control groups. $P<0.05$ was considered statistically significant.

Results

Effects of DMDD on Proliferation in 4T1 Cells

The MTT assay showed that DMDD significantly inhibited the proliferation of 4T1 cells compared with the control group (Figure 2A). The IC_{50} of DMDD treatment for 24 hours of 4T1 cells was 9.95 μM, and the IC_{50} for 48 hours was 6.80 μM. Therefore, the concentrations of 6.8 and 10 μM (as L, M, and H concentration) with 24 hours' treatment on 4T1 cells were used for the following experiments. Furthermore, the result of the clone formation experiment showed that DMDD significantly reduced the number of cell colonies (Figure 2B and C).

Effect of DMDD on Apoptosis in 4T1 Cells

AO/EB assay showed that the cells were mainly normal in the control group, which showed that the cell structure was intact, and the size was normal, and cells are stained with AO in a uniform green. A small number of early apoptotic cells dyed by yellow-green fluorescence were observed in the DMDD L group, which showed that the staining of the cells was enhanced. In the DMDD M and H groups, the normal cells decreased, and the apoptotic cells increased. The late apoptotic cells were observed; these cells were stained with EB to be orange-red. The cell volumes were reduced, and some of the nuclei were ruptured, which showed as fluorescent-stained fragments or plum-shaped nuclei with varying sizes and irregular shapes (Figure 3A). The results of flow cytometry to detect apoptosis rate showed 23.06% of the cells produced apoptosis in the DMDD L group. 46.16% of the cells produced apoptosis in the DMDD M group. 54.32% of the cells produced apoptosis in the DMDD H group. The results further confirmed that DMDD promotes apoptosis of 4T1 cells (Figure 3B).

Effect of DMDD on Cell Cycle in the 4T1 Cells

Cell cycle detection experiment showed with the increase of DMDD concentration, the number of 4T1 cells in the G1 phase gradually raised, and the number of cells in the S/G2 phase gradually decreased (Figure 4A and B). This result suggested that DMDD significantly induced a G1-phase cell-cycle arrest of 4T1 cells.

Effect of DMDD on Migration in 4T1 Cells

A scratch test was used to determine cell migration ability. The result showed the migration ability of 4T1 cells was significantly inhibited, and with the increase of DMDD concentration, the cell migration rate decreased gradually (Figure 5A and B).

Effect of DMDD on Invasion in 4T1 Cells

The result of Matrigel-based transwell assay showed the number of invasive cells in the DMDD group was significantly reduced, and as the concentration of DMDD increased, the number of invading cells gradually decreased (Figure 5C and D). The results indicate that DMDD can weaken the invasive ability of 4T1 cells.

Effect of DMDD on MAPK Signaling Pathway of 4T1 Cells

The result of Relative quantitative real-time PCR showed that DMDD could significantly reduce the gene expressions of raf1, mek1, mek2, erk1, erk2 in 4T1 cells compared with the control group. Also, DMDD significantly

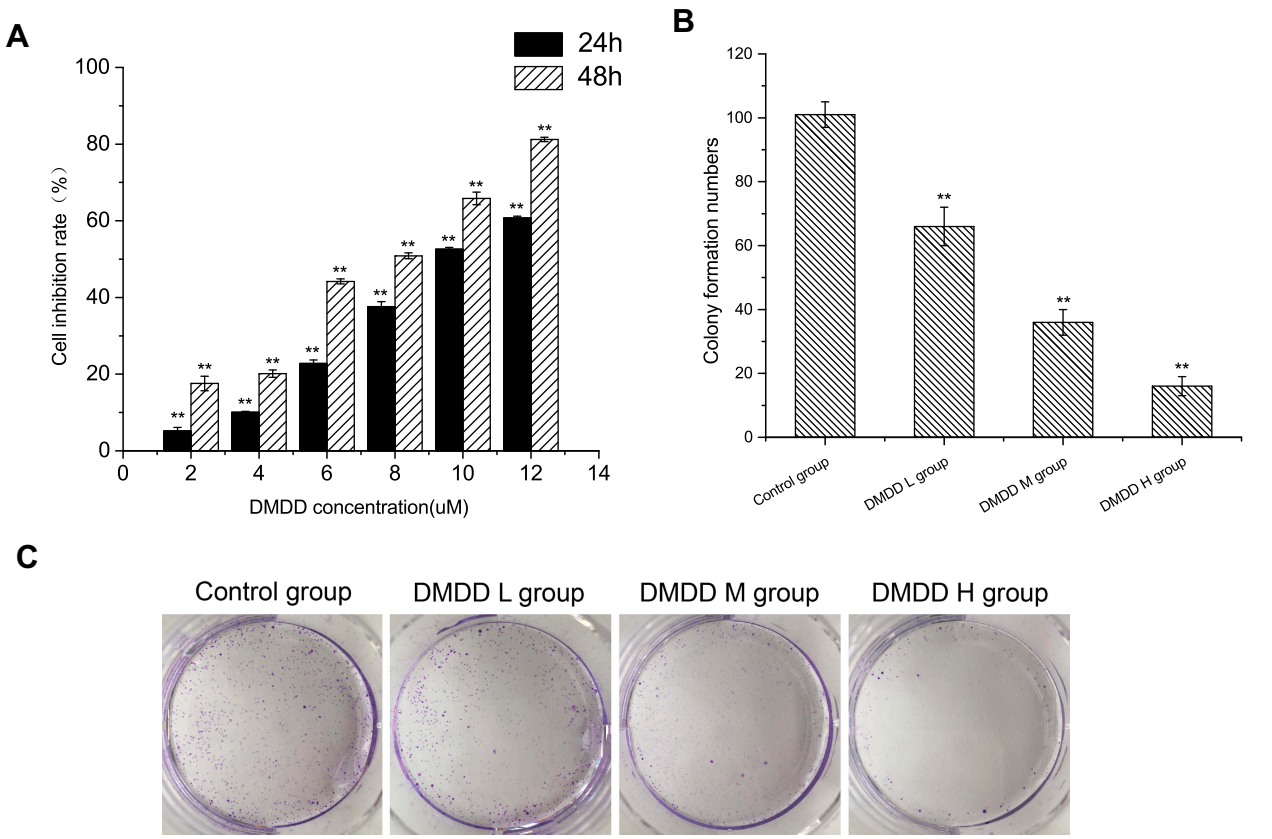

Figure 2 Effect of DMDD on proliferation of 4T1 cells.
Notes: (**A**) 4T1 cells were treated with DMDD (0–12μM) for 24 and 48 hours and the inhibition rates of cell proliferation were detected by MTT assay. (**B**) The clone formation of 4T1 cells treated with DMDD for 24 hours. (**C**) Representative images for the cell colony formation assay. Data are presented as mean ± SD of three experiments. (**P < 0.01, DMDD vs control.) DMDD L group: 6 μM; DMDD M group: 8 μM; DMDD H group: 10 μM.

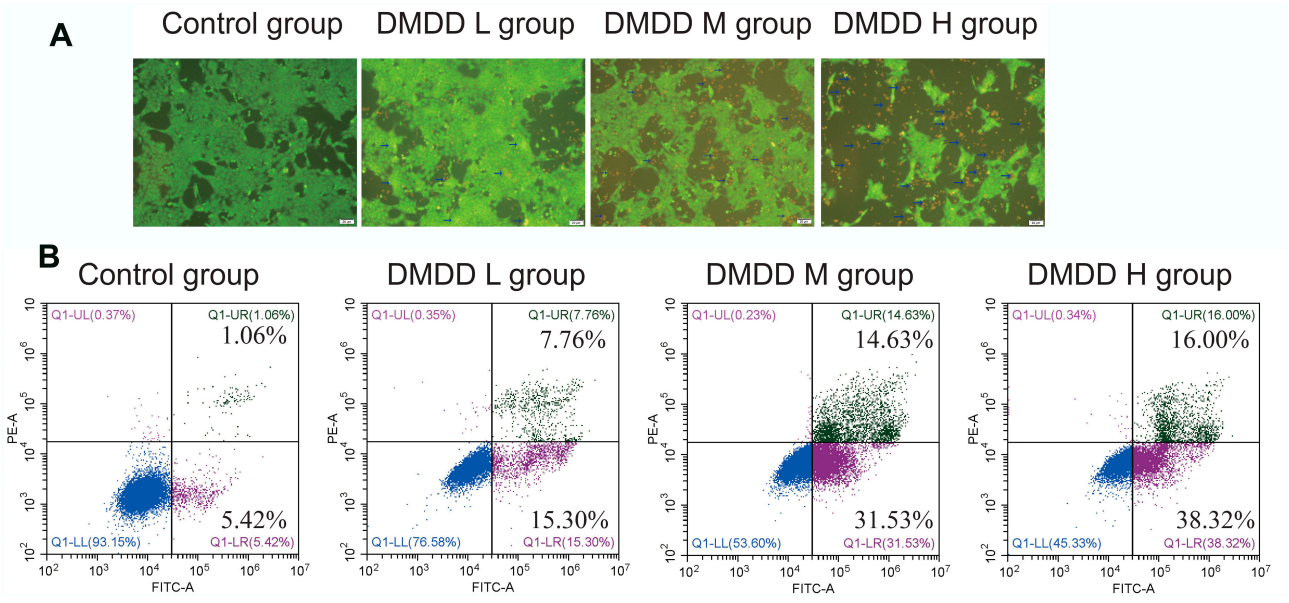

Figure 3 Effect of DMDD on apoptosis of 4T1 cells.
Notes: (**A**) Morphological changes of 4T1 cells treated with DMDD for 24 hours were examined by AO/EB dual staining. (**B**) 4T1 cells were treated with different concentrations of DMDD for 24 hours. The rates of cell apoptosis were evaluated by a flow cytometer. DMDD L group: 6 μM; DMDD M group: 8 μM; DMDD H group: 10 μM.

A

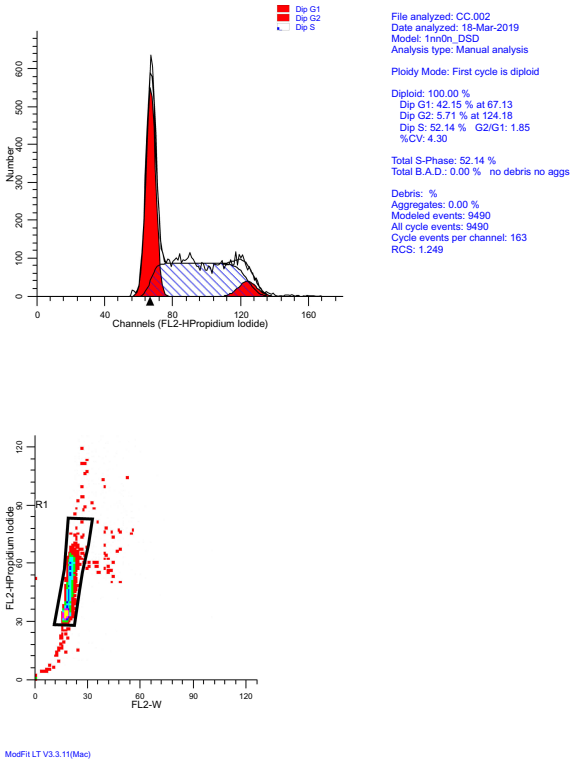

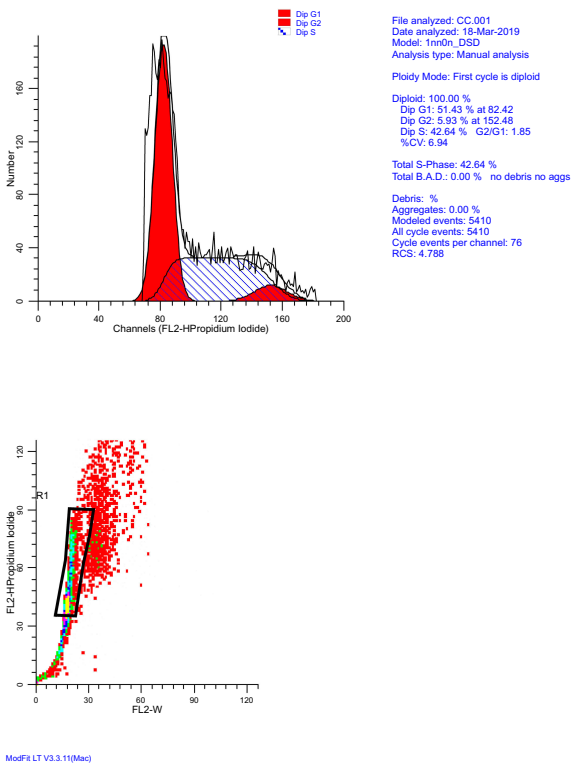

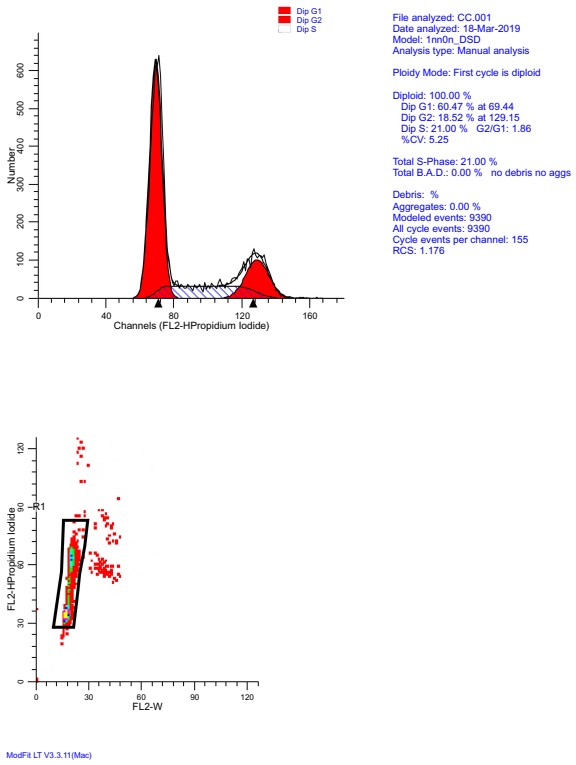

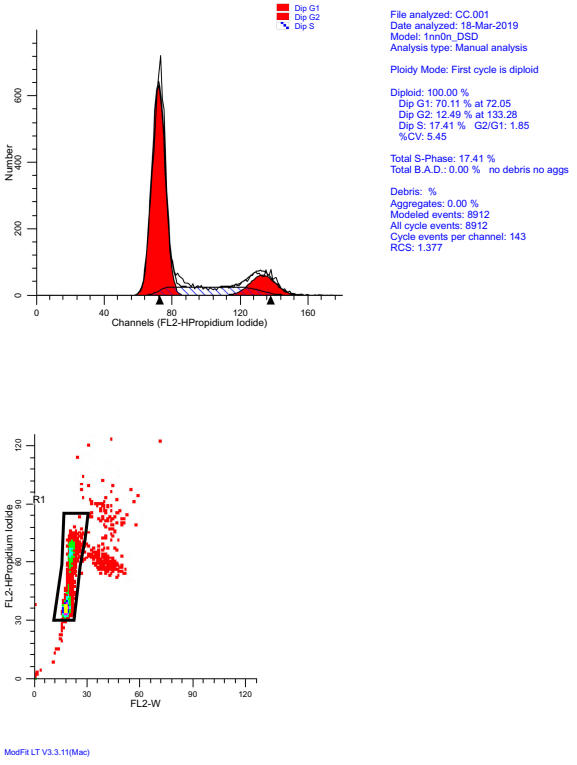

Figure 4 Continued.

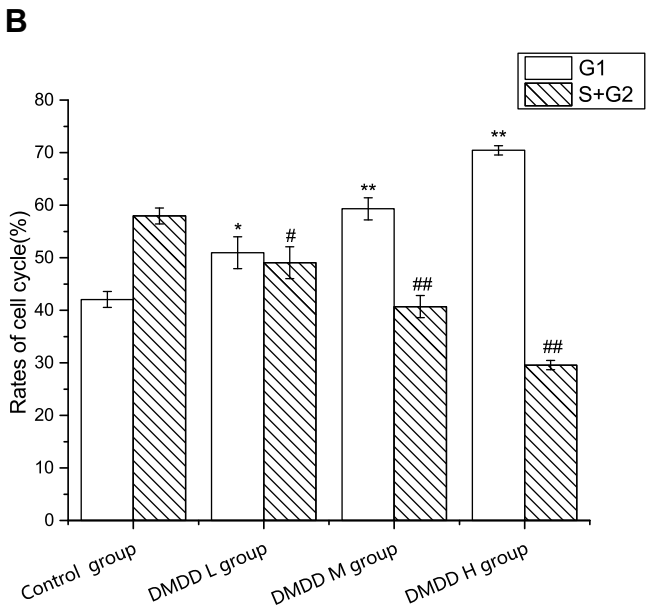

Figure 4 Effect of DMDD on cell cycle of 4T1 cells.
Notes: (**A** and **B**) Effect of DMDD on 4T1 cell cycle. 4T1 cells were treated with different concentrations of DMDD for 24 hours. The cells were collected and dyed with a PI solution. The cell cycle distribution was determined by flow cytometry. Data are presented as mean ± SD of three experiments. *P <0.05, **P < 0.01 (DMDD vs control, Percentages of cell numbers in the G1 phase compared with the control group) $^{\#}p<0.05$, $^{\#\#}p<0.01$ (DMDD vs control, Percentages of cell numbers in the S/G2 phases compared with the control group) DMDD L group: 6 μM; DMDD M group: 8 μM; DMDD H group: 10 μM.

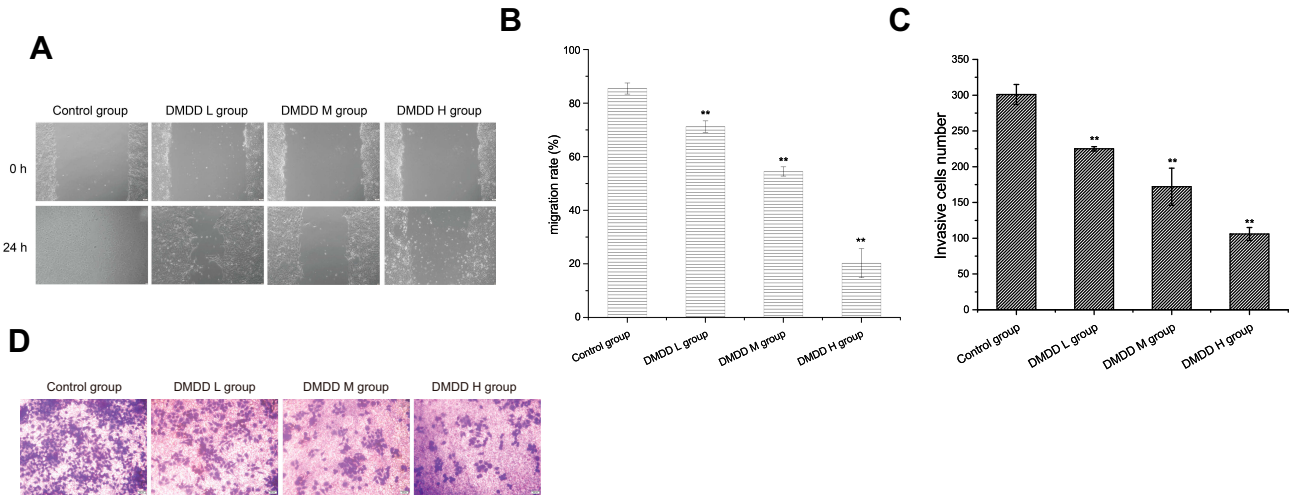

Figure 5 Effect of DMDD on migration and invasion of 4T1 cells.
Notes: (**A** and **B**) The migration rates of 4T1 cells treated with DMDD for 24 hours were detected by the Scratch test. (**C** and **D**) The number of invasive 4T1 cells treated with DMDD for 24 hours was detected by Transwell assay. Data are presented as mean ± SD of three experiments. **P < 0.01, DMDD vs control). DMDD L group: 6 μM; DMDD M group: 8 μM; DMDD H group: 10 μM.

reduced the gene expression of bcl2 in 4T1 cells and increased the gene expression of bax in 4T1 cells (Figure 6A). In the result of Western blot analysis, compared with the control group, DMDD decrease protein expressions of p-raf1, p-mek, p-erk, p-p38, and increased protein expression of p-JNK in 4T1 cells. Furthermore, results showed that DMDD reduced protein expressions of Bcl2, MMP2, and MMP9 and increased the protein expression of Bax in 4T1 cells in a concentration-dependent manner (Figure 6B–L).

DMDD Inhibits Tumor Growth in Breast Cancer Mice

The success rate of the xenograft model of breast cancer in mice was 100%. Tumor nodules appeared at

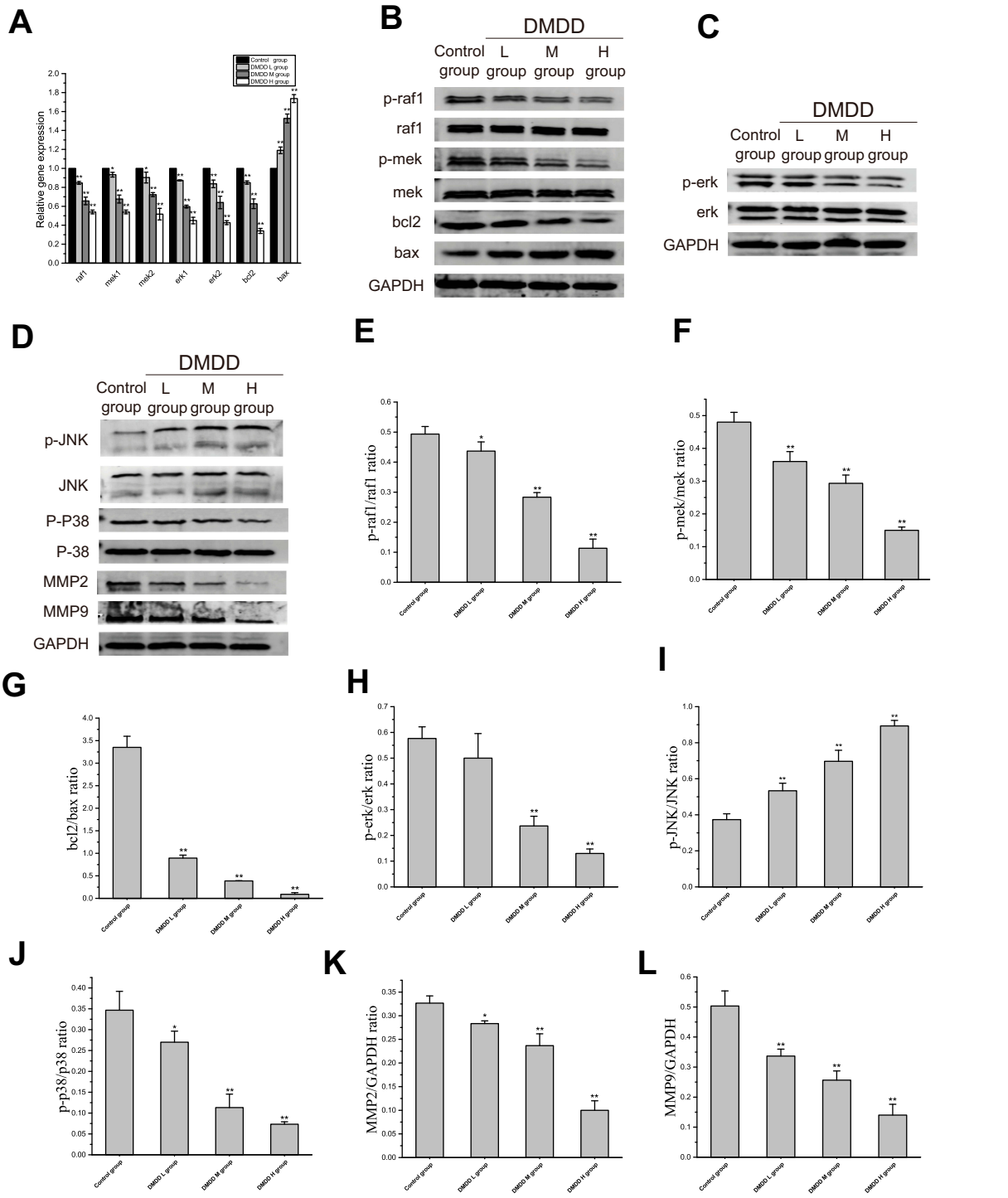

Figure 6 Effect of DMDD on MAPK signaling pathway of 4T1 cells.

Notes: (**A**) Relative quantitative real-time PCR analysis was applied to investigate related gene expressions. (**B**–**L**) Western blot analysis was applied to detect related protein expressions. (**B**) Because the bands of protein p-raf1, raf, p-mek, mek, bcl2, bax, GAPDH were carried out at the same time on different SDS-PAGE gels under the same experimental conditions (include the same batch of protein, the same amount of loading, the same conditions for electrophoresis and transfer, etc.). So they are sharing the same GAPDH. (**D**) Because the bands of protein P-JNK, JNK, P-P38, P38, MMP2, MMP9, GAPDH were carried out at the same time on different SDS-PAGE gels under the same experimental conditions (including the same batch of protein, the same amount of loading, the same conditions for electrophoresis and transfer, etc.). So they are sharing the same GAPDH. Data are presented as mean ± SD of three experiments. (*P < 0.05, **P < 0.01, DMDD vs control). DMDD L group: 6 μM; DMDD M group: 8 μM; DMDD H group: 10 μM.

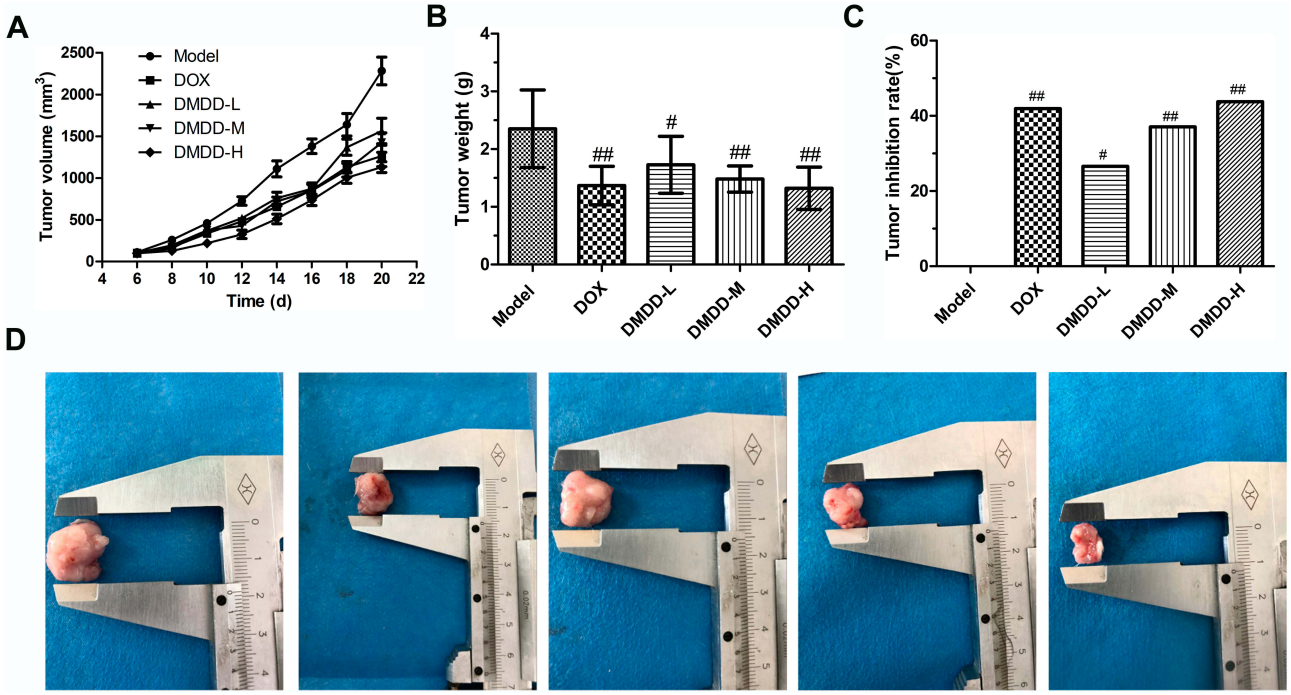

Figure 7 DMDD inhibits tumor growth in vivo.
Notes: (**A**) The tumor volume curve after treatment. (**B**) The tumor weight decreased and (**C**) and the inhibitory rate increased after treatment with CTX and the different doses of DMDD. The tumors are exhibited in (**D**). Data are presented as mean ± SD of three experiments, n=10. ($^{\#}P < 0.05$, $^{\#\#}P < 0.01$, DMDD vs model group).

approximately the fourth day, and most of the tumors reached 100 mm^3. The tumor volumes in the DMDD and DOX groups slowly increased and not exceed 1600 mm^3. The tumors grew to a greater size in the model group, with an average volume of 1978.41 mm^3 (Figure 7A). The tumor weight of the drug group was significantly lower than that of the model group (Figure 7B). The tumor inhibition rates for the DOX, DMDD-L, DMDD-M and DMDD-H groups were 41.9%, 26.59%, 37.06% and 43.8% respectively (Figure 7C). The tumor mass had lobes near the ball, which was light pink or white, with obvious blood vessels. The large tumor mass had a thick texture, and the small tumor mass was soft (Figure 7D).

Effect of DMDD on IL-2, IL-4 and IL-10 Levels in Serum of Mice with Breast Cancer

The results indicated that DMDD could increase the expression of IL-2 compared with the normal, DOX and model groups. While DMDD could decrease the levels of IL-4 and IL-10 compared with the model group (Figure 8).

The Effect of DMDD on Pathological Changes In Breast Cancer Mice Models

HE staining of tumor tissues was carried out in the experiment to preliminarily explore the effect of DMDD on the apoptosis of tumor tissues. In the model group, tumor cells were closely arranged and

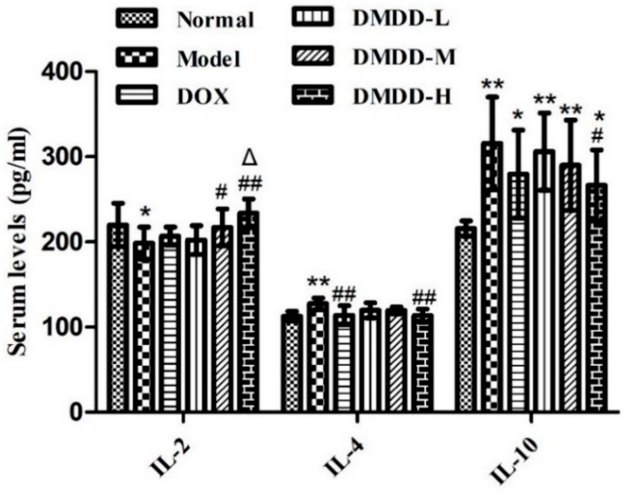

Figure 8 The effect of DMDD on cytokines in breast cancer mice. Data are presented as mean ± SD of three experiments, n=10. ($^{*}P < 0.05$, $^{**}P < 0.01$, DMDD vs normal group; $^{\#}P < 0.05$, $^{\#\#}P < 0.01$, DMDD-H vs model group; $^{\Delta}P < 0.05$, DMDD vs DOX group).

large in size, with diverse nuclei, obvious nucleoli and deep staining. In the HE results of DOX group and DMDD group, there were different degrees of cell apoptosis: loose tumor cell arrangement, decreased number of apoptotic cells, cell membrane shrinkage, decreased volume, nuclear condensation and chromatin aggregation. The pathological results were shown in (Figure 9).

Effect of DMDD on the Ultrastructure of Transplanted Tumors by TEM

In order to further explore the effect of DMDD on the apoptosis of tumor tissues, the microstructure of tumor tissues was observed. The TEM results suggested that the transplanted tumor groups treated with DMDD presented typical apoptosis characteristics. Tumor cells in the model group had large nuclei, obvious nucleoli and complete

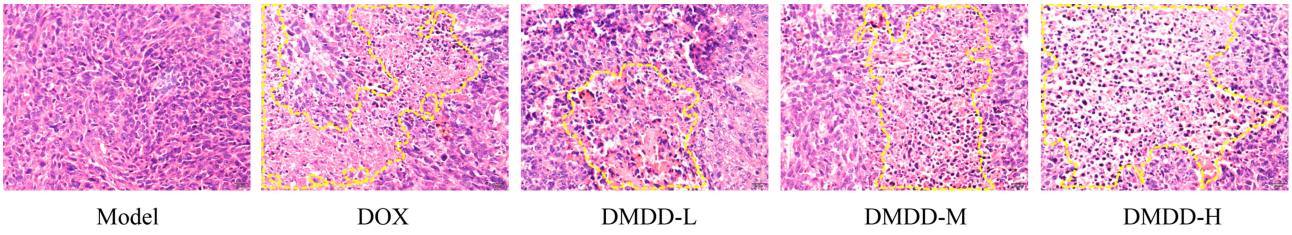

Figure 9 HE staining of breast cancer tumor tissues. Yellow circles: apoptotic tumor. The magnification in A was 400×.

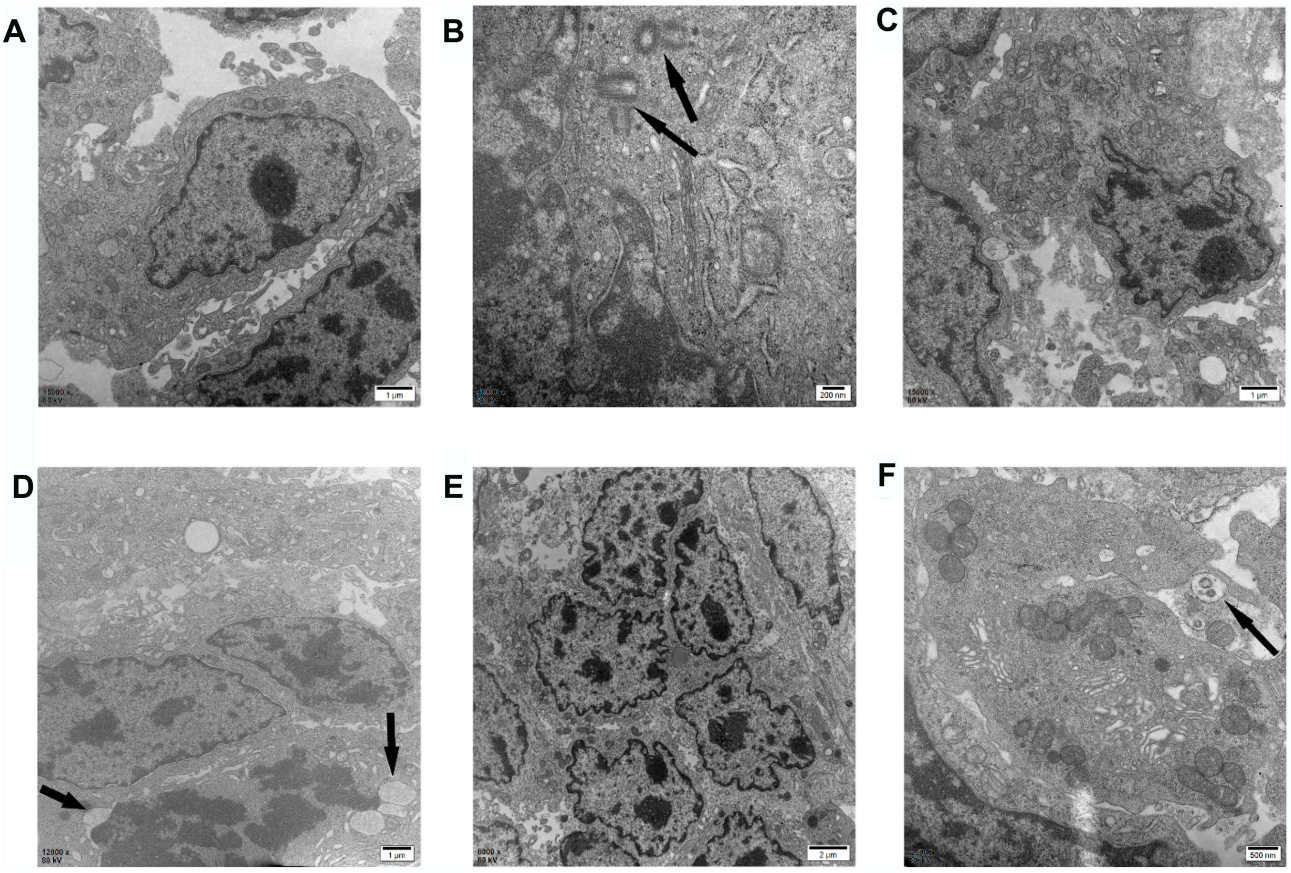

Figure 10 The tumor tissues of breast cancer were observed by TEM.
Notes: (**A** and **B**) The ultrastructure of the tumor in the model group, the black arrows in figure B represent: the centrosome that has completed self-replication in the prophase of cell division. (**C** and **D**) The ultrastructure of the tumor in the DOX group, the black arrows in (**D**) represent: cell nucleus fragmentation membrane foaming. (**E** and **F**). The ultrastructure of the tumor in DMDD-H group, the black arrows in (**F**) represent: free apoptotic body.

organelles. The centrosome in the prophase of mitosis was also detected, and self-replication was completed. Apoptotic characteristics were observed in the DOX group, including nuclear condensation, heterochromatin agglutination and marginalization (Figure 10A and B). In addition, fragmented membrane bubbles appeared in the nucleus (Figure 10C and D). Clear nuclear condensation, chromatin agglutination, cell wrinkling and fragmentation appeared in the DMDD-H group, and free apoptotic bodies were also observed (Figure 10E and F).

DMDD Promotes Cell Apoptosis in Tumor Tissues

To further confirm the apoptotic ability of DMDD induced tumor cells, TUNEL staining of tumor tissues was performed. TUNEL staining micrographs showed that the number of cells with DNA fragmentation increased in the groups treated with DMDD. The highest number of cells with fragmented DNA was observed in the DMDD-H group compared to the values observed in the other groups (Figure 11A). The percentages of TUNEL-positive cells in the model, DOX, DMDD-L, DMDD-M, DMDD-H groups were 5.07±2.90%, 44.41 ±20.01%, 27.28±8.48%, 46.06±19.49%, and 65.43 ±10.48%, respectively (Figure 11B).

Effect of DMDD on Expression of Related Genes

To explore the underlying mechanisms by which DMDD inhibits tumor growth and promotes the apoptosis of breast cancer cells in mice, the expression of genes involved in the cancer-associated MAPK signaling and apoptotic pathways was assessed, including RAF1, MEK1/2, ERK1/2, Bax and Bcl-2. An obvious decrease in the levels of RAF1, MEK1/2 and ERK1/2 expression was observed in the DMDD and DOX groups compared with the levels of these factors observed in the model group (Figure 12A–E). Bax mRNA expression was notably upregulated, whereas the expression of Bcl-2 mRNA was downregulated in the DMDD and DOX groups (Figure 12F and G).

Effect of DMDD on the Expression of Related Protein Expression by IHC

On the basis of gene results, the MAPK pathway-related proteins were detected by immunohistochemistry, and semi-quantitative analysis was conducted.

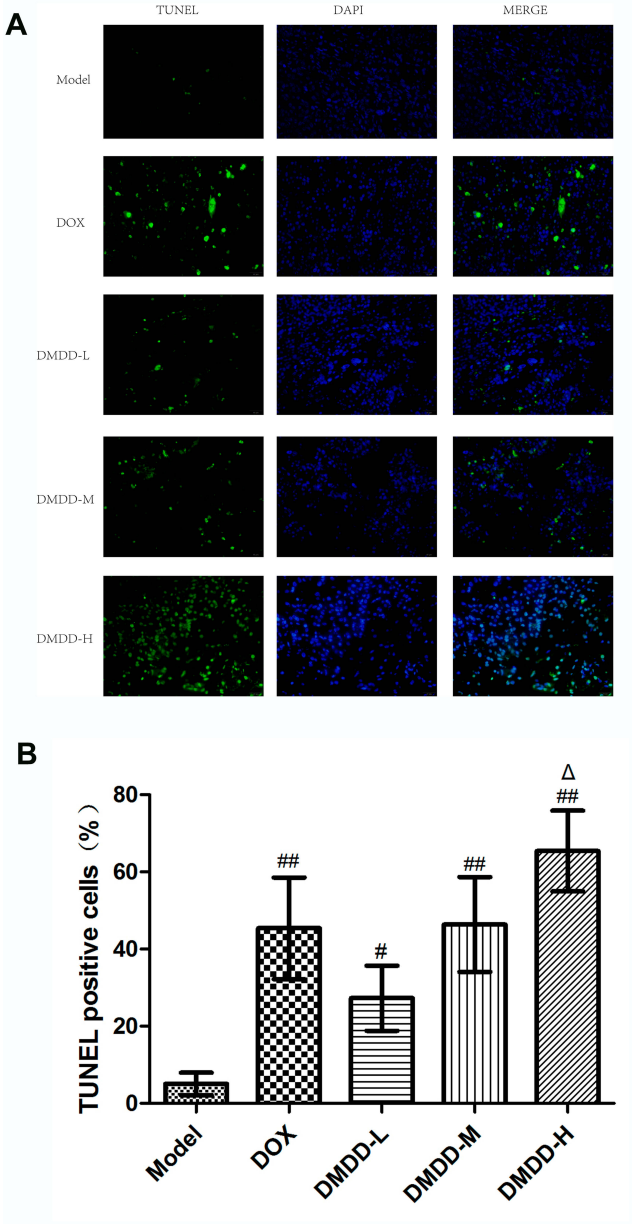

Figure 11 TUNEL results in tumor tissue from breast cancer.
Notes: (**A**) Microscopic observation of TUNEL results (magnification: 400×). (**B**) Results of TUNEL-positive cell apoptosis rate. Data are presented as mean ± SD of three experiments, n=3. ($^{\#}P < 0.05$, $^{\#\#}P < 0.01$, DMDD vs model group; $^{\Delta}P < 0.05$, DMDD-H vs DOX group).

The expression of p-RAF1, p-MEK and p-ERK in tumor tissues was assessed by IHC. The positive expression of these proteins was primarily observed in the cytoplasm, and partly in the cell nuclei, which were stained brown and yellow. Compared with the model group, the expression of these three proteins was downregulated in the DMDD and DOX groups (Figure 13 A and B).

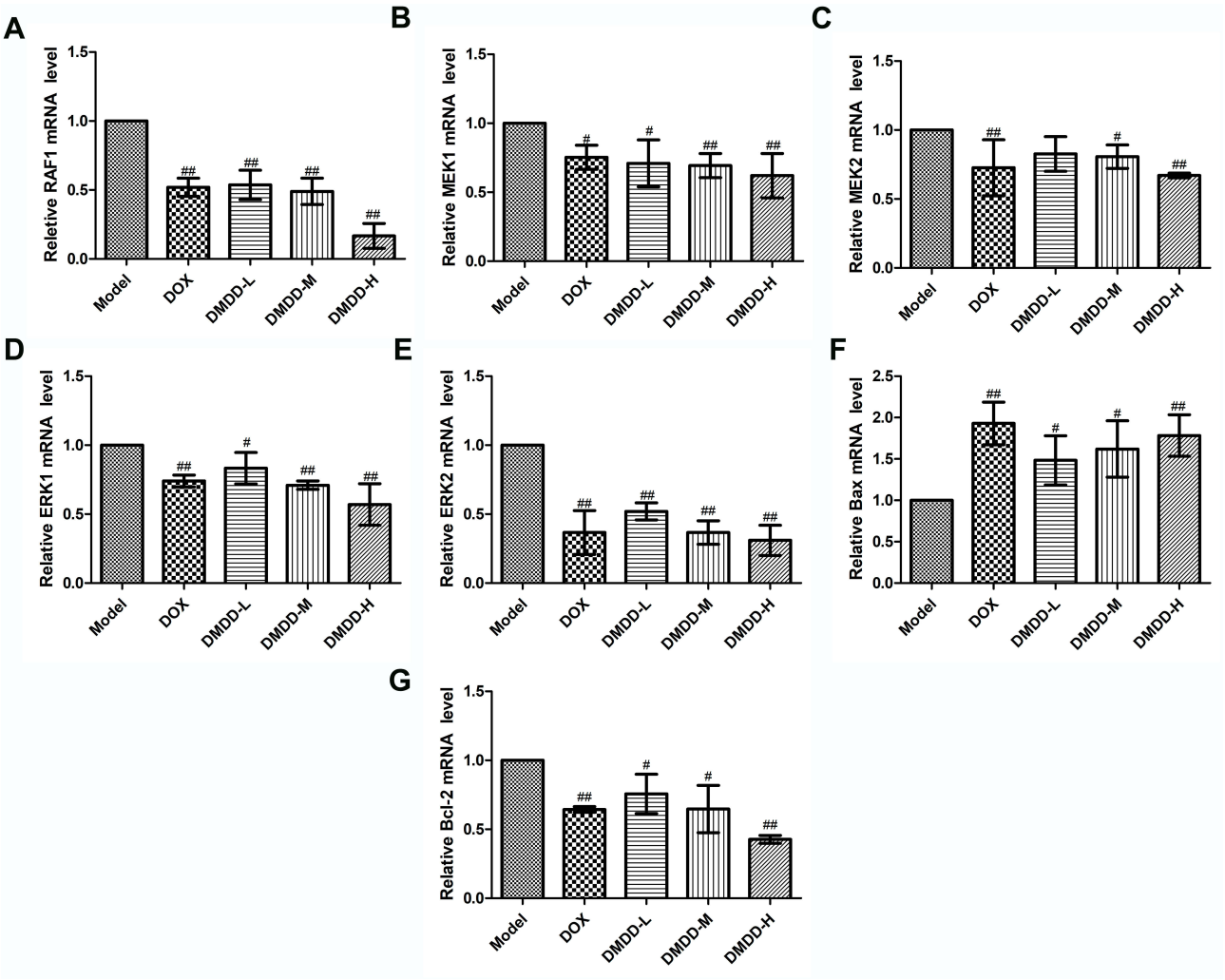

Figure 12 mRNA expressions of MAPK pathway-related genes in breast cancer tumor tissues.
Notes: (**A**–**G**) mRNA expression of RAF1, MEK1, MEK2, ERK1, ERK2, Bax, Bcl-2. Data are presented as mean ± SD of three experiments, n=3. ($^{\#}P < 0.05$, $^{\#\#}P < 0.01$, vs model group).

Effect of DMDD on the Expression of MAPK Signaling Pathway-Related Proteins in Mouse Breast Tumors

In the result of Western blot analysis, compared with the model group, the protein expressions of p-RAF1, p-MEK, p-ERK and p-P38 were significantly decreased in the DMDD and DOX treatment groups (Figure 14A–H). Furthermore, for the apoptotic proteins, the results showed that DMDD could significantly upregulate the expression of Bax and downregulate the expression of Bcl-2 compared with that observed in the model group (Figure 14I–L).

Discussion

Breast cancer remains a global problem that threatens women's health. Clinically, anticancer drugs for the treatment of breast cancer have many adverse reactions.[24] Thus, it is important and necessary to research and develop a new anticancer drug that is highly effective and of low toxicity. In recent years, tumor epidemiology research has found that the isolation of effective anti-cancer active ingredients from plants has attracted more and more attention from scholars and is a hot spot for cancer prevention and treatment. DMDD is a compound extracted and isolated from the roots of Averrhoa carambola L and is patented. In recent years, our research team found that DMDD can inhibit the proliferation of various tumor cell lines in vitro, especially breast cancer cells. The studies of Zheng et al[8] also confirmed that DMDD did not cause any acute toxicity in the acute toxicity experiment of mice. Therefore, DMDD might be an antitumor candidate that is effective with low toxicity.

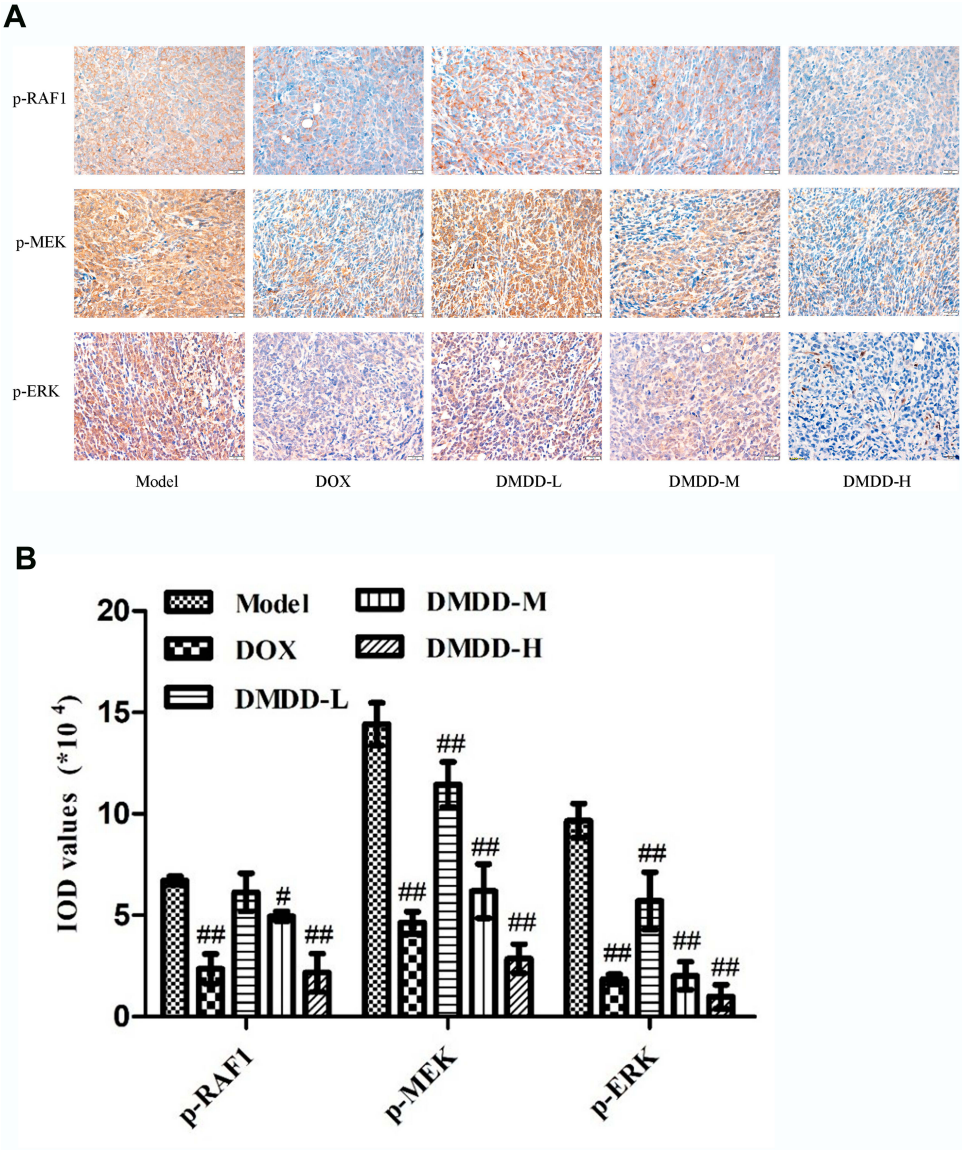

Figure 13 Immunohistochemical results of breast cancer tumor tissue.
Notes: (**A**) Immunohistochemical map of tumor tissue (magnification: 400×). (**B**) IOD expression levels of p-RAF1, p-MEK and p-ERK.Data are presented as mean ± SD of three experiments, n=3. ($^{\#}P < 0.05$, $^{\#\#}P < 0.01$, vs model group).

Inducing apoptosis in tumor cells is one of the targets for the development of anticancer drugs. Apoptosis, programmed cell death, plays a key role in maintaining a balance between cell proliferation and death. The mitochondrial pathway is one of the apoptotic pathways. The Bcl-2 family is one of the key elements that influences the ability of the mitochondrial pathway to regulate apoptosis.[25] Bcl-2 and Bax proteins as the two major regulators of apoptosis in the Bcl-2 family are functionally opposite.[26,27] Studies have shown tumor cell apoptosis is closely related to the pathway of MAPK. In the researches of AO/EB staining analysis and cell apoptosis analysis, DMDD significantly induced apoptosis of 4T1 cells. Also, PCR and WB experiments showed that DMDD decreased the expression levels of the Bcl2 gene and protein, and DMDD increased the expression levels of Bax gene and protein, thereby inducing apoptosis of 4T1 cells.

Two important stages in the cell cycle are G1 phase to S phase, and G2 phase to M phase, and they are the transitional period's molecular change. Signal transduction pathway-associated regulatory genes can regulate cell proliferation, division, and differentiation in the cell cycle. Many important anti-tumor mechanisms are inhibiting cell proliferation by affecting the cell cycle.[28] The results of

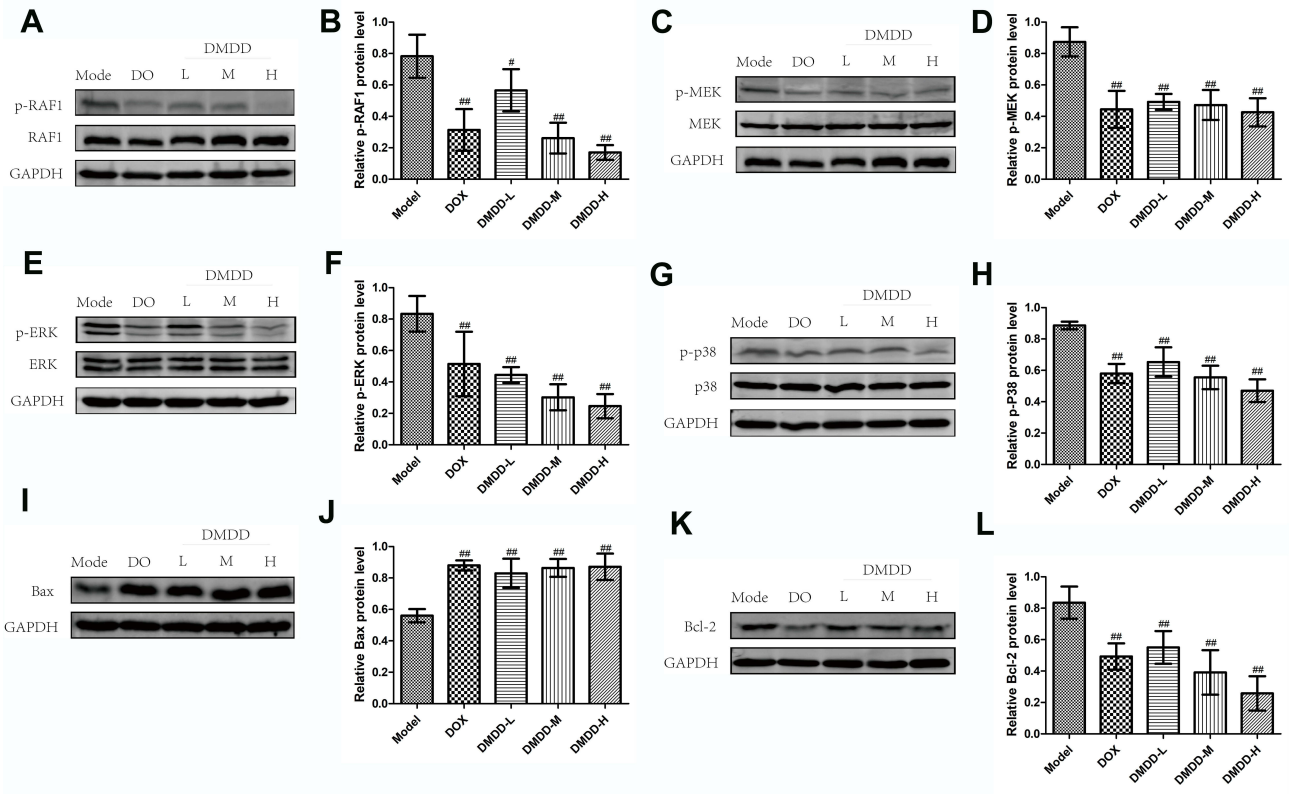

Figure 14 Detection results of MAPK pathway-related proteins in breast cancer tumor tissues.
Notes: (**A**–**L**) The WB image and relative protein expression of p-RAF1, p-MEK, p-ERK, p-P38, Bax and Bcl-2. Data are presented as mean ± SD of three experiments, n=3. ($^{\#}P < 0.05$, $^{\#\#}P < 0.01$, vs model group).

cell cycle analysis showed that DMDD induce G1-phase cell cycle arrest.

In this study, the results of tumor size, tumor weight and tumor inhibition rate analyses showed that DMDD could effectively inhibit the growth of breast cancer in mice and the effect was dose-dependent.

Interleukin has been widely used in clinical research including cancer as a regulator of immune response. Il-2 is a multipotent cytokine in cellular immune response, which can promote the growth of T cells and enhance the natural killing ability.[29,30] There were studies that showed that Il-2 had been successfully used in the treatment of cancer because it promoted the secretion of T cells and NK cells.[31] IL-4 and IL-10 are important participants in the humoral immune response, but they play an immunosuppressive role in the cellular immune response. Studies have shown that IL-4 and IL-10 can be used as diffuse gastric tumor molecular markers that distinguish□stage and □ stage of cancer, was advantageous to the control of cancer.[32] In this experiment, the expression of IL-2 in the model group was lower than that in the normal group, indicating that the expression of IL-2 in breast cancer in the untreated mice was low, while that in the DOX group and the DMDD group were both higher than that in the model group, and the expression of IL-2 in the DMDD-H group was higher than that in the DOX group, indicating that DMDD could effectively improve the expression of IL-2. The expression of IL-4 and IL-10 in solid tumor mice was higher than that in normal mice, and the expression of IL-4 and IL-10 in each drug group was lower than that in the model group. These results showed that DMDD increased the level of IL-2 and decreased the expression of IL-4 and IL-10, suggesting that DMDD enhanced the immune function of breast cancer mice to inhibit tumor growth.

Apoptosis is an active death process controlled by genes. Some studies have shown that the change of apoptosis was not only related to the occurrence and development of tumor but also related to the drug resistance of tumor.[33] The pro-apoptotic effect of DMDD was studied by HE staining, TEM observation and TUNEL staining. The results of HE staining showed that the cancer cells in the model group were closely arranged, large in size and obvious in nucleoli, while the HE results in the DOX group and the DMDD group showed different degrees of apoptosis: fewer cells, looser in arrangement, smaller in

size and nuclear fixation, indicating that DMDD could induce apoptosis of breast cancer cells in mice. TEM is used to observe the microstructure of tumor tissue. We found that the nucleus, nucleolus and organelles in the the model group are complete. DOX and DMDD-H groups have typical apoptosis characteristics. The results confirmed that DMDD promote tumor cell apoptosis from the microscopic view. e The TUNEL staining was quantitatively analyzed in the experiment, and the results showed that the positive apoptotic cell rate of DOX group and DMDD group was higher than that of the model group, and the apoptotic cell rate of DMDD-H group was the highest, which further indicated that DMDD could increase the number of tumor cell apoptosis. These three experiments fully confirmed that DMDD can effectively induce apoptosis of breast cancer cells and play an anticancer role.

MAPKs cascade activation is central to many signaling pathways. It is an important molecule that receives the signal transduction and transmission of membrane receptors and brings them into the nucleus. It plays a key role in many cell proliferation-related signaling pathways. When the cells do not receive any stimulations, MAPKs are at rest. After cells receive stimulation of cells by growth factors or other factors, MAPKs are activated or inhibited, which are characterized by progressive phosphorylation.[34,35] Activation or inhibition of the MAPK signaling pathway plays an important role in regulating tumor cell proliferation, differentiation, and apoptosis.[20] In our study, WB analysis displayed DMDD significantly inhibited the expressions of p-raf1, p-erk, p-mek, p-p38 in 4T1 cells and tumor tissue. Also, the level of protein Bax was up-regulated, and the level of protein Bcl2 was down-regulated.

Furthermore, studies have shown that the MAPK signaling pathway is closely related to invasion and metastasis of tumor cells.[36] MMPs degrade the protein ingredients in the extracellular matrix and damage the histological barrier of cancer cell invasion. MMP2 and MMP9 are important matrix metalloproteinases, which mainly degrade type IV collagen and play an important role in tumor migration and invasion.[37] In our studies, the scratch test and Transwell assay showed that DMDD could attenuate the abilities of migration and invasion in 4T1 cells. Western blot displayed DMDD can significantly down-regulate the expression levels of MMP2 and MMP9 in 4T1 cells, thereby inhibiting the migration and invasion of 4T1 cells.

Conclusion

DMDD has a good anti-tumor effect on breast cancer in vivo and in vitro. The mechanism may be related to the regulation of the MAPK signaling pathway, thereby regulating the expression of downstream target proteins Bcl2, Bax, MMP2, and MMP9 to exert anti-tumor effects.

Funding

This research was funded by the Guangxi Key Laboratory of Bio-targeted Diagnosis and Treatment Research (GXSWBX201804), the Natural Science Foundation of China (81760665, 81460205) and Guangxi First-class Discipline Project for Pharmaceutical Sciences (No. GXFCDP-PS-2018).

Disclosure

The authors state that there is no conflict of interest in this work.

References

1. De Pergola G, Giagulli VA, Bartolomeo N, et al. Independent relationship between serum osteocalcin and uric acid in a cohort of apparently healthy obese subjects. *Endocr Metab Immune Disord Drug Targets*. 2017;17(3):207–212. doi:10.2174/1871530317666170825164415
2. Siegel RL, Miller KD, Jemal A. Cancer statistics, 2018. *CA Cancer J Clin*. 2018;68(1):7–30. doi:10.3322/caac.21442
3. Mi B, Yu C, Pan D, et al. Pilot prospective evaluation of (18)F-alfatide II for detection of skeletal metastases. *Theranostics*. 2015;5(10):1115–1121. doi:10.7150/thno.12938
4. Yu Z, Zhang T, Zhou F, et al. Anticancer activity of Saponins from Allium chinense against the B16 melanoma and 4T1 breast carcinoma cell. *Evid Based Complement Alternat Med*. 2015;2015:725023. doi:10.1155/2015/725023
5. Fu Z, Lin L, Liu S, et al. Ginkgo biloba extract inhibits metastasis and ERK/nuclear factor kappa B (NF-κB) signaling pathway in gastric cancer. *Med Sci Monit*. 2019;25(11):6836–6845. doi:10.12659/MSM.915146
6. Xie W, Zhang Y, Zhang S, et al. Oxymatrine enhanced anti-tumor effects of Bevacizumab against triple-negative breast cancer via abating Wnt/β-Catenin signaling pathway. *Am J Cancer Res*. 2019;9(8):1796–1814.
7. Wen Q, Lin X, Liu Y, et al. Phenolic and lignan glycosides from the butanol extract of Averrhoa carambola L. root. *Molecules*. 2012;17(10):12330–12340. doi:10.3390/molecules171012330
8. Zheng N, Lin X, Wen Q, et al. Effect of 2-dodecyl-6-methoxycyclohexa-2,5-diene-1,4- dione, isolated from Averrhoa carambola L. (Oxalidaceae) roots, on advanced glycation end-product-mediated renal injury in type 2diabetic KKAy mice. *Toxicol Lett*. 2013;219(1):77–84. doi:10.1016/j.toxlet.2013.03.001
9. Xu X, Liang T, Wen Q, et al. Protective effects of total extracts of Averrhoa carambola L. (Oxalidaceae) roots on streptozotocin-induced diabetic mice. *Cell Physiol Biochem*. 2014;33(5):1272–1282. doi:10.1159/000358695
10. Xie Q, Zhang S, Chen C, et al. Protective effect of 2-dodecyl-6-oxycycloh exa-2,5-diene-1,4-dione, isolated from Averrhoa Carambola L., against palmitic acid-induced inflammation and apoptosis in Min6 Cells by inhibiting the TLR4-MyD88-NF-kappa B signaling pathway. *Cell Physiol Biochem*. 2016;39(5):1705–1715. doi:10.1159/000447871

11. Li J, Wei X, Xie Q, et al. Protective Effects of 2-Dodecyl-6-Methoxycyclohexa-2,5 -Diene-1,4-Dione Isolated from *Averrhoa Carambola* L. (*Oxalidaceae*) roots on high-fat diet-induced obesity and insulin resistance in mice. *Cell Physiol Biochem*. 2016;40 (5):993–1004. doi:10.1159/000453156
12. Gao Y, Huang R, Gong Y, et al. The antidiabetic compound 2-dodecyl-6-methoxycyclohexa −2,5-diene-1,4-dione, isolated from Averrhoa carambola L., demonstrates significant antitumor potential against human breast cancer cells. *Oncotarget*. 2015;6(27):24304–24319. doi:10.18632/oncotarget.4475
13. Chen C, Nong Z, Xie Q, et al. 2-Dodecyl-6- methoxycyclohexa −2,5-diene-1,4-dione inhibits the growth and metastasis of breast carcinoma in mice. *Sci Rep*. 2017;7(1):6704.
14. Hu KH, Li WX, Sun MY, et al. Cadmium-induced apoptosis in MG63 cells by increasing ROS, activation of p38 MAPK and inhibition of ERK 1/2 pathways. *Cell Physiol Biochem*. 2015;36(2):642–654. doi:10.1159/000430127
15. Kim EK, Choi EJ. Pathological roles of MAPK signaling pathways in human diseases. *Biochim Biophys Acta Mol Basis Dis*. 2010;1802 (4):396–405. doi:10.1016/j.bbadis.2009.12.009
16. Blüthgen N, Legewie S. Systems analysis of MAPK signal transduction. *Essays Biochem*. 2008;45:95–107. doi:10.1042/BSE0450095
17. Junttila MR, Li SP, Westermarck J. Phosphatase-mediated crosstalk between MAPK signaling pathways in the regulation of cell survival. *FASEB J*. 2008;22(4):954–965. doi:10.1096/fj.06-7859rev
18. Cuevas BD, Abell AN, Johnson GL. Role of mitogen-activated protein kinase kinase kinases in signal integration. *Oncogene*. 2007;26(22):3159–3171. doi:10.1038/sj.onc.1210409
19. Su L, Chen X, Wu J, et al. Galangin inhibits proliferation of hepatocellular carcinoma cells by inducing endoplasmic reticulum stress. *Food Chem Toxicol*. 2013;62:810–816. doi:10.1016/j.fct.2013.10.019
20. Guarino M. Src signaling in cancer invasion. *J Cell Physiol*. 2010;223(1):14.
21. Sebolt-Leopold JS. Advances in the development of cancer therapeutics directed against the RAS-mitogen-activated protein kinase pathway. *Clin Cancer Res*. 2008;14(12):3651–3656.
22. Song L, Liu D, Zhao Y, et al. Sinomenine inhibits breast cancer cell invasion and migration by suppressing NF-κB activation mediated by IL-4/miR-324-5p /CUEDC2 axis. *Biochem Biophys Res Commun*. 2015;464(3):705. doi:10.1016/j.bbrc.2015.07.004
23. Ding QX, Li Z, Yang Y, et al. Preparation and therapeutic application of docetaxel-loaded poly(D, L-lactide) nanofibers in preventing breast cancer recurrence. *Drug Deliv*. 2015;7(23):1.
24. Hassan AHE, Choi E, Yoon YM, et al. Natural products hybrids: 3,5,4′-trimethoxystilbene– 5,6,7-trimethoxyflavone chimeric analogs as potential cytotoxic agents against diverse human cancer cells. *Eur J Med Chem*. 2019;161:559–580. doi:10.1016/j.ejmech.2018.10.062
25. Dong X, Fu J, Yin X, et al. Induction of apoptosis in HepaRG cell line by Aloe-Emodin through generation of reactive oxygen species and the mitochondrial pathway. *Cell Physiol Biochem*. 2017;42 (2):685–696. doi:10.1159/000477886
26. Birkinshaw RW, Czabotar PE. The BCL-2 family of proteins and mitochondrial outer membrane permeabilisation. *Semin Cell Dev Biol*. 2017;72:152–162. doi:10.1016/j.semcdb.2017.04.001
27. Tang H, Wei W, Wang W, et al. Effects of culturedCordyceps mycelia polysaccharide A on tumor neurosis factor-alpha induced hepatocyte injury with mitochondrial abnormality. *Carbohydr Polym*. 2017;163: 43–53.
28. PARK JW, CHOI YJ, JANG MA, et al. Chemopreventive agent resveratrol, a natural product derived from grapes, reversibly inhibits progression through S and G2 phases of the cell cycle in U937 cells. *Cancer Lett*. 2001;163(1):43–49. doi:10.1016/S0304-3835(00)00658-3
29. Song N, Han S, Lee K, et al. Genetic Variants in Interleukin-2 and Risk of Lymphoma among Children in Korea. *Asian Pac J Cancer Prev*. 2012;13(2):621–623. doi:10.7314/APJCP.2012.13.2.621
30. Ren G, Tian G, Liu Y, et al. Recombinant newcastle disease virus encoding IL-12 and/or IL-2 as potential candidate for hepatoma carcinoma therapy. *Technol Cancer Res Treat*. 2016;15(5):P83–P94. doi:10.1177/1533034615601521
31. Sun Z, Ren Z, Yang K, et al. Author Correction: a next-generation tumor-targeting IL-2 preferentially promotes tumor-infiltrating CD8 (+) T-cell response and effective tumor control. *Nat Commun*. 2020;11(1):1716. doi:10.1038/s41467-020-15532-1
32. Orea MAD, Perez VM, Conde EG, et al. Expression of cytokines interleukin-2, interleukin-4, interleukin-10 and transforming growth factor β in gastric adenocarcinoma biopsies obtained from Mexican patients. *Asian Pac J Cancer Prev*. 2017;18(2):577–582.
33. Hashemzaei M, Far AD, Yari A, et al. Anticancer and apoptosis-inducing effects of quercetin in vitro and in vivo. *Oncol Rep*. 2017;38 (2):819–828. doi:10.3892/or.2017.5766
34. Cargnello M, Roux PP. Activation and function of the MAPKs and their substrates, the MAPK-activated protein kinases. *Microbiol Mol Biol Rev*. 2011;75(1):50–83. doi:10.1128/MMBR.00031-10
35. Wada T, Penninger JM. Mitogen-activated protein kinases in apoptosis regulation. *Oncogene*. 2004;23(16):2838–2849. doi:10.1038/sj.onc.1207556
36. LIN MT, Lin BR, Chang CC, et al. IL-6 induces AGS gastric cancer cell invasion via activation of the c-Src/□hoA/□OCK signaling pathway. *Int J Cancer*. 2007;120(12):2600. doi:10.1002/ijc.22599
37. Cheng TC, Din ZH, Su JH, et al. Sinulariolide suppresses cell migration and invasion by inhibiting matrix metalloproteinase-2/-9 and urokinase through the PI3K/AKT/mTOR signaling pathway in human bladder cancer cells. *Mar Drugs*. 2017;15(8):pii: E238. doi:10.3390/md15080238